# N-terminal domain of PB1-F2 protein of influenza A virus can fold into amyloid-like oligomers and damage cholesterol and cardiolipid containing membranes

Dalila Ajjaji, Charles-Adrien Richard, Sandra Mazerat, Christophe Chevalier, Jasmina Vidic

# N-terminal domain of PB1-F2 protein of influenza A virus can fold into amyloid-like oligomers and damage cholesterol and cardiolipid containing membranes

Ajjaji, Dalila; Richard, Charles-Adrien; Mazerat, Sandra; Chevalier, Christophe; Vidic, Jasmina

2016

Ajjaji, D., Richard, C.-A., Mazerat, S., Chevalier, C., & Vidic, J. (2016). N-terminal domain of PB1-F2 protein of influenza A virus can fold into amyloid-like oligomers and damage cholesterol and cardiolipid containing membranes. Biochemical and Biophysical Research Communications, 477(1), 27-32.

https://hdl.handle.net/10356/81154

https://doi.org/10.1016/j.bbrc.2016.06.016

# N-terminal domain of PB1-F2 Protein of Influenza A Virus can Fold into Amyloid-like Oligomers and Damage Cholesterol and Cardiolipid Containing Membranes

Dalila Ajjaji[1,2], Charles-Adrien Richard[1], Sandra Mazerat[3], Christophe Chevalier[1*] and Jasmina Vidic[1,4*]

[1]Virologie et Immunologie Moléculaires, UR892, INRA, Paris Saclay University, 78350 Jouy en Josas, France.

2 Laboratoire de Physique Statistique, École Normale Supérieure, 24 rue Lhomond, 75005 Paris, France

3 Institut de Chimie Moléculaire et des Matériaux d'Orsay, Université Paris-Sud, CNRS, UMR 8182, 91400 Orsay, France.

[4]Nanyang Technological University-Hebrew University of Jerusalem-Ben Gurion University, NEW CREATE, Singapore 138602.

**Corresponding Authors:**

*Dr J. Vidic, E-mail: jasmina.vidic@jouy.inra.fr

Dr C. Chevalier, E-mail: christophe.chevalier@jouy.inra.fr

Virologie et Immunologie Moléculaires, UR892, INRA, Paris Saclay University, 78350 Jouy en Josas, France.

Tel.: (+33) 134 652623; Fax: (+33) 134652621

**ABSTRACT**

PB1-F2 protein is a factor of virulence of influenza A viruses which increases the mortality and morbidity associated with infection. Most seasonal H1N1 Influenza A viruses express nowadays a truncated version of PB1-F2. Here we show that truncation of PB1-F2 modified supramolecular organization of the protein in a membrane-mimicking environment. In addition, full-length PB1-F2(1-90) and C-terminal PB1-F2 domain (53-90), efficiently permeabilized various anionic liposomes while N-terminal domain PB1-F2(1-52) only lysed cholesterol and cardiolipin containing lipid bilayers. These findings suggest that the truncation of PB1-F2 may impact the pathogenicity of a given virus strain.

KEYWORDS:

PB1-F2-membrane interaction; Influenza A viruses; Amyloid-like protein structures; Cholesterol; Cardiolipin.

## 1. Introduction

Every year, seasonal Influenza A viruses (IAV) affect millions of people leading to illness and death. Moreover, highly pathogenic influenza strains represent a constant global public health concern [1,2]. PB1-F2 is an accessory IAV protein encoded by an alternative +1 open

reading frame of the PB1 viral segment. PB1-F2 was first described as a pro-apoptotic factor causing cell death and having others unknown functions contributing to the virulence [3,4,5]. PB1-F2 activities were shown to be associated with compromising mitochondria function [6,7], down-regulation the host immune response [3,7], enhancing PB1 activity[8] and rising risk of secondary bacterial infections [9].

Most avian IAV strains express a full-length PB1-F2 protein of 90 amino acids [4,10] The three influenza viruses responsible of the main pandemics over the last century in 1918, 1957 and 1968 also expressed the full-length protein [5]. In contrast, the 2009 H1N1 pandemic influenza virus did not encode functional PB1-F2 (only an 11 amino acid form) [11]. Indeed, since 1949 most human H1N1 expressed C-terminal truncated forms of the PB1-F2 [5]. Isolates of recent H7N9 strains express truncated forms of PB1-F2 [12] which suggests that avian virus adaption to mammalian host lead to the deletion of PB1-F2 function.

Although non-structured in aqueous solutions, PB1-F2 adopts to a β-sheet conformation and oligomerizes to amyloid-like structures in an anionic membrane-mimicking environment [13,14,15]. We have shown that cytotoxicity caused by PB1-F2 is triggered by the protein soluble amyloid structures [14]. PB1-F2 aggregates were detected in the context of IAV infected cells [13,15,16] which additionally suggests that toxic PB1-F2 oligomers contribute to the virus pathogenicity. Here, we compared the abilities of a 52-amino acid form of PB1-F2 to assemble into amyloid-like structures in a membrane-mimicking environment and to compromise membrane integrity.

## 2. Materials and Methods

*2.1. PB1-F2 expression and purification*

PB1-F2 protein of A/WSN/1933 (H1N1) influenza virus was used in this study. The gene encoding full-length PB1-F2(1-90) protein was cloned into pET 22b+ expression vector (Novagen), and the gene en-coding N-terminal part of PB1-F2 (1-52) was cloned into pET28 in order to express His-tagged proteins. Induction transformed BL-21 Rosetta cells (Stratagene) was performed by addition of 1 mM isopropyl 1-thio-B-D-galactopyranoside for 4 hours at 37°C. After cells were lysed and inclusion bodies containing the recombinant PB1-F2-His proteins were solubilized in 8M urea buffer. Proteins from inclusion bodies were purified on a 5mL Hitrap-IMAC column using AKTA Purifier-100 FPLC chromatographic system (GE Healthcare). Fractions collected containing PB1-F2-His proteins were further purified by size exclusion chromatography on a 120mL HiLoad Superdex 200 column. This two-step purification procedure allowed to obtain highly purified protein samples as illustrated in Supplementary Fig. 1A and B.

C-terminal domain of PB1-F2(53-90) was custom made by Proteogenix (France). Prior to analysis lyophilized protein powder was dissolved in 10 mM sodium actete buffer and its concentration was de-termined by measuring optical density at 280 nm using extinction coefficient deduced from its composition of 28990 $M^{-1}cm^{-1}$, 5500 $M^{-1}cm^{-1}$ and 4833 $M^{-1}cm^{-1}$ for PB1-F2(1-90), PB1-F2(1-52) and PB1-F2(53-90), respectively.

*2.2.Reagents*

Phosphatidylserine (PS) and Phosphatidylcholine (PC) were purchased from Avanti Polar Lipids (AL, USA). Other reagents were purchased from Sigma-Aldrich (France).

*2.3. Liposomes preparation and permeabilization assay*

Liposomes of various lipid compositions were prepared as previously described 1. All liposomes used in this study were extruded through a polycarbonate membrane filter (MILLIPORE 0.1 µm) to obtain unilamellar vesicles of environ 100 nm diameter.

For the leakage measurements, 35 mM calcein (Calcein disodium salt, Fluka) was dropped inside lipo-somes as explained previously 1,2. Calcein efflux measurements were performed on a Tecan microplate reader using 96 plates. Measurements were performed in a 160 µl volume containing 0.01 mg/ml lipo-somes in the sodium acetate buffer pH 5. The ability of proteins to permeabilize liposomes was monitored by continuous measuring of calcein fluorescence emission at 528 nm upon excitation at 492 nm. The fluorescence intensity was normalized regarding the signal intensity obtained by the addition of 0.1 % (v/v) Triton X100 to the liposome preparation. All runs were done at least in triplicate and were found to be in close agreement.

*2.4.Circular Dichroism Spectroscopy*

Far-UV (180-260 nm) circular dichroism (CD) spectra were measured on a JASCO J-810 spectropolar-imeter using 1 mm path length quartz cell. Spectra were collected at a scanning rate of 100 nm/min, with a band width of 1.0 nm and a resolution of 100 mdeg and corrected for the contribution of the buffer. Each spectrum was an average of 8 scans. Measurements were done at 20°. CD spectra were analyzed and quantified using the DicroWeb software.

*2.5.Tryptophan fluorescence measurements*

Fluorescence measurements were performed with a FP-6200 spectrofluorimeter (JASCO, Tokyo, Japon) connected with a thermostatted cell holder at 20 °C, using a 1-cm path length quartz cell. PB1-F2 (2 µM) was incubated with 0.001% w/v SDS or LUVs in different concentrations ranging from 0.01 to 0.5 mg/ml in 10 mM sodium-acetate buffer for 24 hrs before measurements. The fluorescent spectra were acquired in the range of 290 to 450 nm when excited at 280 nm, at a scanning rate 125 nm/min, and a bandwidth 5 nm.

*2.6. DLS analysis*

Dynamic Light Scattering (DLS) measurements were performed on a Zetasizer Nano serie (Malvern, UK). The scattering intensity data were processed using the instrumental software to obtain the hydro-dynamic diameter (RH) and the size distribution of particles in each sample. RH of the particles was es-timated from the autocorrelation function, using the Cumulants method. A total of 10 scans with an overall duration of 5 min were obtained for each sample. All measurements were done in at 20 °C.

*2.7.AFM*

A commercial dimension 3100 AFM (Vecco Instruments, USA) was used for topographical characteri-zation of the samples. All measurements were performed at the tapping mode using rectangular silicon AFM tip.

### 3. Results and discussion

Full length PB1-F2(1-90) converts from random into amyloid-like structures in a diluted solution of anionic detergent SDS (concentration of SDS below its CMC of 0.23 %$_{w/v}$) [13,15,17]. To determine if PB1-F2 (1-52) and PB1-F2 (53-90) also convert into amyloid-like structures, the proteins were dissolved in 10 mM sodium-acetate buffer, pH 5 containing 0.05 %$_{v/w}$ SDS. All measurements were done at pH 5 since PB1-F2 precipitates at physiological pH [13,14]. Firstly, we measured the proteins intrinsic fluorescent emission upon excitation of their Trp residues at 292 nm. Among the five Trps of PB1-F2, four are located within its C-terminal domain (Trp58, 61, 80 and 88), and one within the N- terminal domain (Trp9). The $\lambda_{max}$ of fluorescence emission of Trp reflects the polarity of its environment. In hydrophilic solutions, the $\lambda_{max}$ can reach 355 nm, while in hydrophobic environments, i.e. when the Trp is located within the protein structured domains, the $\lambda_{max}$ shifts to 320 nm. In the absence of SDS, $\lambda_{max}$ of all three PB1-F2 constructs reached 356 nm (Fig. 1A), indicating that Trps are fully exposed to hydrophilic buffer solvent. This was expected for unstructured proteins in an aqueous solution. In 0.05 % $_{w/v}$. SDS solution, the $\lambda_{max}$ of all three proteins blue shifted to 342 nm (Fig. 1A). This significant shift of 14 nm, indicates that Trp residues became less exposed to the hydrophilic solvent upon addition of SDS suggesting that proteins had folded into more ordered structures.

Moreover, full length PB1-F2 showed a decrease in Trp fluorescence intensity at $\lambda_{max}$ suggesting that the gain of structure was accompanied by a partial protein precipitation. This was expected since full length PB1-F2 was shown to form amyloid aggregates of different sizes in a diluted SDS solution [13,15]. In contrast, the fluorescent intensity at $\lambda_{max}$ of PB1-F2(53-90) increased,

while the Trp fluorescence of PB1-F2(1-52) rested almost unchanged in the presence of SDS compared to what was observed in the buffer alone. Thus, truncated PB1-F2 probably assembled into small soluble structures in a diluted SDS solution.

To estimate the size of protein assemblies formed in a diluted SDS solution, DLS measurements were performed. Proteins were incubated within a 0.005 %w/v. SDS in 10 mM sodium acetate buffer, pH 5, and their hydrodynamic diameters ($R_H$) were continuously measured within a few hours (Fig. 1B). Without SDS, the estimated $R_H$ of PB1-F2 is 1 - 10 nm [13,14]. Such sizes are expected for a small non-structured protein of molecular mass of about 10 kDa. Upon the addition of SDS, oligomers were rapidly formed as $R_H$ of all three proteins instantly reached several hundred nm (Fig. 1B). At ~ 60 min of incubation $R_H$ of PB1-F2 (1-52) and PB1-F2 (53-90) increased to 400 nm, while the $R_H$ of full-length PB1-F2 dramatically increased to reach 2-3 µm. Findings in Fig.1B strongly suggest that all three proteins self-associated rapidly to oligomerized species upon addition of SDS. Within 60-minutes, full-length PB1-F2 polymerized further to larger polymers in the micron size range. In contrast, truncated PB1-F2 only formed small aggregates in membrane mimicking environment within this time scale.

Next we investigated the amyloid feature of SDS-induced assemblies of PB1-F2. The ThT fluorescent signal was measured continuously in PB1-F2 solutions upon addition of 0.005 % w/v. SDS. We had previously reported that neither full length nor truncated PB1-F2 proteins formed ThT positive structures in an aqueous solution, pH 5 [14]. In the presence of SDS, PB1-F2 (1-52) and PB1-F2 (53-90) were found to display a similar slope and saturation time of ThT signal increase (Fig. 1C). No lag phase, generally assigned to protein nucleation, was observed at the beginning of the linear part of the graphs. However, late intensity saturation of ThT

fluorescent signal of full-length compared to those of truncated PB1-F2 was observed (10 min for PB1-F2 (1-52) and PB1-F2 (53-90) and 30 min for the full-length PB1-F2) (Fig. 1C). In addition, 3-fold higher slope of the polymerization rate was found for full-length PB1-F2 (33°) compared to PB1-F2 (1-52) and PB1-F2 (53-90) (11°) (Fig. 1C). ThT binds to amyloid structures of different sizes with similar affinities [18] and thus its signal intensity cannot indicate the type of amyloid structures formed. However, the slope of ThT signal increase determined by real time measurement reflects the kinetics of the amyloid formation. Different slope obtained for full length PB1-F2 polymerization compared to those observed for truncated proteins corresponds to distinct kinetics of protein polymerizations. This probably came from the formation of various type of amyloid structures by three PB1-F2 forms, which is in agreement with previous observations [13,15].

To visualize molecular assemblies formed in a diluted SDS solution, AFM analysis was performed on full-length and truncated PB1-F2 preparations. The AFM images of full-length PB-F2 revealed the presence of bundles of intertwined fibrils of several µm in length and diameter between 1.5 and 10 nm (Fig. 1D). Observed sizes are similar to those published for amyloid fibers formed by other proteins [19,20]. However, the real size of PB1-F2 fibers in SDS solution may be underestimated since AFM was done on samples dried under mild condition to facilitate their adhesion to the substrate. Drying can dehydrate and deform amyloid filaments as reported before [21,22]. AFM imaging of PB1-F2 (53-90) incubated with SDS showed two types of aggregated structures: predominant small unfused particles, which can be assigned to oligomers, and few long fibrils. Filaments formed by PB1-F2 (53-90) were of irregular structure and looked more like connected oligomers than steady polymeric fiber (Fig. 1D). In contrast, AFM images of ThT-positive entities formed by PB1-F2 (1-52) in the presence of SDS were of globular

spherical-shapes (Fig. 1D). No N-terminal PB1-F2 fibrils were observed. AFM visualization confirmed that in membrane-mimicking environment only full-length PB1-F2 fibrillated into long amyloid filaments.

The propensity of a protein to form amyloid structures is frequently correlated to its toxicity, since amyloids disturb cell membrane integrity [23]. In the context of infection, PB1-F2 was shown to accumulate as soluble amyloid oligomers in the membrane vicinity [13,15,16].

Thus, we compared the lytic activities of full-length and truncated PB1-F2. PB1-F2 and notably its C-terminus lyse anionic but not neutral lipid bilayers [14,24,25]. Importantly, N-terminal domain of PB1-F2 was shown to have no lytic activity towards both neutral and negatively charged membranes [14]. Hence, we wondered if specific lipids such as cholesterol or cardiolipin may modulate PB1-F2 lytic activities.

Cholesterol is a critical structural component of lipid raft domains that plays functional roles in many aspects of the influenza A virus life cycle. We prepared PC/cholesterol liposomes (14:1 molar ratio) and add to the suspension PB1-F2 (1-90), PB1-F2 (1-52) or PB1-F2 (53-90) at concentrations ranging from 2 nM to 1000 nM. For all PB1-F2 forms, the presence of cholesterol significantly increased the dye released as compared to those observed with neutral PC liposomes (Fig. 2). For instance, 1 µM of full-length PB1-F2 permeabilized 70 % of PC/Cholesterol liposomes against only 20 % of PC liposomes. Positive effect of cholesterol on PB1-F2 lysis activity may be explained by the negative charge of cholesterol which facilitates electrostatic interactions between liposomes and positively charged PB1-F2 proteins. Alternatively cholesterol may facilitate PB1-F2 membrane destabilization by modifying membrane fluidity [26]. When cholesterol was added to negatively charged vesicles (PC/PS/Cholesterol, 9:4:1 molar ratio), different effects were observed for the three protein

constructs: cholesterol partially inhibited lysis efficiency of PB1-F2 (52-90), but facilitated that of PB1-F2 (1-52). Cholesterol had no significant effect on full-length PB1-F2 permeabilizing activity. Similarly, no cholesterol effect was observed previously when full-length PB1-F2 interaction with planar lipid membranes was studied [24]. Surprisingly, the N-terminal part of PB1-F2 completely lysed PC/PS/cholesterol liposomes at concentration of 1 µM. This suggests that N-terminal part of PB1-F2 may destabilize membranes containing sterol rafts.

Next, membrane leakage was monitored with vesicles containing cardiolipin. The cardiolipin is almost exclusively localized in the inner mitochondrial membrane where it is involved in mitochondrial membrane dynamics and the mitochondrial apoptotic process [27]. P1-F2 was shown to particularly interact with the inner mitochondrial membrane to perforate lipid bilayers causing cytochrome c release [28]. The % dye released from liposomes containing PC/cardiolipin (2:1, molar ratio) treated with PB1-F2, PB1-F2 (1-52) or PB1-F2 (53-90) were similar to those found in pure PC liposomes (Fig. 2). In contrast, presence of cardiolipin in negatively charged liposomes (PC/PS/cardiolipin, 1:1:1 molar ratio) significantly increased the leakage effects of N-terminal domain and full-length PB1-F2 (Fig. 2). At concentration of 500 nM the full-length PB1-F2 completely destabilized PC/PS/Cardiolipin liposomes within 30 min. Surprisingly, a partial inhibitory effect of cardiolipin was evidenced on lysis activity of PB1-F2(53-90) in PC/PS/Cardiolipin (1:1:1, molar ratio) liposomes compared to PC/PS ones (1:1 molar ration).

Overall our results suggested that incubation in an anionic membrane-mimicking environment resulted distinct kinetics of polymerization for full-length, N- and C-terminal domains of PB1-F2 to fold into different supramolecular organizations. Full-length PB1-F2 (1-90) and PB1-F2 (53-90) efficiently disrupted various anionic synthetic membrane, while PB1-F2

(1-52) only lysed cholesterol or cardiolipin containing membranes. Most PB1-F2 function as apoptosis induction [6,8,25], infected cell necrosis [14], modulation of host cell response [29] and increased lethality in mice [30,31] are associated with its C-terminal part. Our data support that N-terminal domain of PB1-F2 shows no tendency to polymerize into amyloid fibers in an anionic membrane-like environment, which contrast the full length protein. Nevertheless, PB1-F2 (1-52) may efficiently damage membranes containing cholesterol and cardiolipin. However, exactly how is the truncated small PB1-F2 form activity within infection context still has to be studied.

**Notes**

The authors declare no competing financial interests.

**ACKNOWLEDGMENT**

Support for this work came from in-house funding from UR982 of INRA. JV acknowledges travel support from a BioAsia grant 35976PH. We benefited from the facilities of protein purification platform (VIM, INRA) and we thank Dr M. Moudjou (INRA, France) for expert assistance. We thank Dr A. Low Yuen Kei (NTU, Singapore) for proof reading and Dr J.-F. Chich (INRA, France) for helpful discussion.

**REFERENCES**

[1] E.C. Claas, A.D. Osterhaus, R. van Beek, J.C. De Jong, G.F. Rimmelzwaan, D.A. Senne, S. Krauss, K.F. Shortridge, R.G. Webster, Human influenza A H5N1 virus related to a highly pathogenic avian influenza virus, Lancet 351 (1998) 472-477.

[2] R. Gao, B. Cao, Y. Hu, Z. Feng, D. Wang, W. Hu, J. Chen, Z. Jie, H. Qiu, K. Xu, X. Xu, H. Lu, W. Zhu, Z. Gao, N. Xiang, Y. Shen, Z. He, Y. Gu, Z. Zhang, Y. Yang, X. Zhao, L. Zhou, X. Li, S. Zou, Y. Zhang, X. Li, L. Yang, J. Guo, J. Dong, Q. Li, L. Dong, Y. Zhu, T. Bai, S. Wang, P. Hao, W. Yang, Y. Zhang, J. Han, H. Yu, D. Li, G.F. Gao, G. Wu, Y. Wang, Z. Yuan, Y. Shu, Human infection with a novel avian-origin influenza A (H7N9) virus, N Engl J Med 368 (2013) 1888-1897.

[3] W. Chen, P.A. Calvo, D. Malide, J. Gibbs, U. Schubert, I. Bacik, S. Basta, R. O'Neill, J. Schickli, P. Palese, P. Henklein, J.R. Bennink, J.W. Yewdell, A novel influenza A virus mitochondrial protein that induces cell death, Nat Med 7 (2001) 1306-1312.

[4] A. Krumbholz, A. Philipps, H. Oehring, K. Schwarzer, A. Eitner, P. Wutzler, R. Zell, Current knowledge on PB1-F2 of influenza A viruses, Med Microbiol Immunol 200 (2011) 69-75.

[5] A.K. Chakrabarti, G. Pasricha, An insight into the PB1F2 protein and its multifunctional role in enhancing the pathogenicity of the influenza A viruses, Virology 440 (2013) 97-104.

[6] H. Yamada, R. Chounan, Y. Higashi, N. Kurihara, H. Kido, Mitochondrial targeting sequence of the influenza A virus PB1-F2 protein and its function in mitochondria, FEBS Lett 578 (2004) 331-336.

[7] T. Yoshizumi, T. Ichinohe, O. Sasaki, H. Otera, S. Kawabata, K. Mihara, T. Koshiba, Influenza A virus protein PB1-F2 translocates into mitochondria via Tom40 channels and impairs innate immunity, Nat Commun 5 (2014) 4713.

[8] I. Mazur, D. Anhlan, D. Mitzner, L. Wixler, U. Schubert, S. Ludwig, The proapoptotic influenza A virus protein PB1-F2 regulates viral polymerase activity by interaction with the PB1 protein, Cell Microbiol 10 (2008) 1140-1152.

[9] J.L. McAuley, F. Hornung, K.L. Boyd, A.M. Smith, R. McKeon, J. Bennink, J.W. Yewdell, J.A. McCullers, Expression of the 1918 influenza A virus PB1-F2 enhances the pathogenesis of viral and secondary bacterial pneumonia, Cell Host Microbe 2 (2007) 240-249.

[10] A.V. Vasin, O.A. Temkina, V.V. Egorov, S.A. Klotchenko, M.A. Plotnikova, O.I. Kiselev, Molecular mechanisms enhancing the proteome of influenza A viruses: an overview of recently discovered proteins, Virus Res 185 (2014) 53-63.

[11] M. Sarkar, A.S. Agrawal, R. Sharma Dey, S. Chattopadhyay, R. Mullick, P. De, S. Chakrabarti, M. Chawla-Sarkar, Molecular characterization and comparative analysis of pandemic H1N1/2009 strains with co-circulating seasonal H1N1/2009 strains from eastern India, Arch Virol 156 (2011) 207-217.

[12] P. Wei, W. Li, H. Zi, M. Cunningham, Y. Guo, Y. Xuan, T.H. Musa, P. Luo, Epidemiological and molecular characteristics of the PB1-F2 proteins in H7N9 influenza viruses, Jiangsu, Biomed Res Int 2015 (2015) 804731.

[13] C. Chevalier, A. Al Bazzal, J. Vidic, V. Fevrier, C. Bourdieu, E. Bouguyon, R. Le Goffic, J.F. Vautherot, J. Bernard, M. Moudjou, S. Noinville, J.F. Chich, B. Da Costa, H. Rezaei, B. Delmas, PB1-F2 influenza A virus protein adopts a beta-sheet conformation and forms amyloid fibers in membrane environments, J Biol Chem 285 (2010) 13233-13243.

[14] J. Vidic, C.A. Richard, C. Pechoux, B. Da Costa, N. Bertho, S. Mazerat, B. Delmas, C. Chevalier, Amyloid Assemblies of Influenza A Virus PB1-F2 Protein Damage Membrane and Induce Cytotoxicity, J Biol Chem 291 (2016) 739-751.

[15] A. Miodek, J. Vidic, H. Sauriat-Dorizon, C.A. Richard, R. Le Goffic, H. Korri-Youssoufi, C. Chevalier, Electrochemical detection of the oligomerization of PB1-F2 influenza A virus protein in infected cells, Anal Chem 86 (2014) 9098-9105.

[16] C. Chevalier, R. Le Goffic, F. Jamme, O. Leymarie, M. Refregiers, B. Delmas, Synchrotron Infrared and Deep UV Fluorescent Microspectroscopy Study of PB1-F2 beta-Aggregated Structures in Influenza A Virus-Infected Cells, J Biol Chem (2016).

[17] J. Vidic, Le Goffic, R., Miodek, A., Bourdieu, C., Richard, C.A., Moudjou, M., Delmas, B and Chevalier, C., Detection of Soluble Oligomers Formed by PB1-F2 Influenza A Virus Protein in Vitro, J. Anal. Bioanal. Tech. 4 (2013).

[18] M. Biancalana, S. Koide, Molecular mechanism of Thioflavin-T binding to amyloid fibrils, Biochim Biophys Acta 1804 (2010) 1405-1412.

[19] R. Jansen, W. Dzwolak, R. Winter, Amyloidogenic self-assembly of insulin aggregates probed by high resolution atomic force microscopy, Biophys J 88 (2005) 1344-1353.

[20] N. Makarava, V.G. Ostapchenko, R. Savtchenko, I.V. Baskakov, Conformational switching within individual amyloid fibrils, J Biol Chem 284 (2009) 14386-14395.

[21] D.M. Hatters, C.A. MacRaild, R. Daniels, W.S. Gosal, N.H. Thomson, J.A. Jones, J.J. Davis, C.E. MacPhee, C.M. Dobson, G.J. Howlett, The circularization of amyloid fibrils formed by apolipoprotein C-II, Biophys J 85 (2003) 3979-3990.

[22] A. Relini, C. Canale, S. De Stefano, R. Rolandi, S. Giorgetti, M. Stoppini, A. Rossi, F. Fogolari, A. Corazza, G. Esposito, A. Gliozzi, V. Bellotti, Collagen plays an active role in the aggregation of beta2-microglobulin under physiopathological conditions of dialysis-related amyloidosis, J Biol Chem 281 (2006) 16521-16529.

[23] J.E. Straub, D. Thirumalai, Membrane-Protein Interactions Are Key to Understanding Amyloid Formation, J Phys Chem Lett 5 (2014) 633-635.

[24] A.N. Chanturiya, G. Basanez, U. Schubert, P. Henklein, J.W. Yewdell, J. Zimmerberg, PB1-F2, an influenza A virus-encoded proapoptotic mitochondrial protein, creates variably sized pores in planar lipid membranes, J Virol 78 (2004) 6304-6312.

[25] M. Henkel, D. Mitzner, P. Henklein, F.J. Meyer-Almes, A. Moroni, M.L. Difrancesco, L.M. Henkes, M. Kreim, S.M. Kast, U. Schubert, G. Thiel, The proapoptotic influenza A virus protein PB1-F2 forms a nonselective ion channel, PLoS One 5 (2010) e11112.

[26] A. Chabanel, M. Flamm, K.L. Sung, M.M. Lee, D. Schachter, S. Chien, Influence of cholesterol content on red cell membrane viscoelasticity and fluidity, Biophys J 44 (1983) 171-176.

[27] R.H. Houtkooper, F.M. Vaz, Cardiolipin, the heart of mitochondrial metabolism, Cell Mol Life Sci 65 (2008) 2493-2506.

[28] D. Zamarin, A. Garcia-Sastre, X. Xiao, R. Wang, P. Palese, Influenza virus PB1-F2 protein induces cell death through mitochondrial ANT3 and VDAC1, PLoS Pathog 1 (2005) e4.

[29] J.L. McAuley, K. Zhang, J.A. McCullers, The effects of influenza A virus PB1-F2 protein on polymerase activity are strain specific and do not impact pathogenesis, J Virol 84 (2010) 558-564.

[30] A.L. Reis, J.W. McCauley, The influenza virus protein PB1-F2 interacts with IKKbeta and modulates NF-kappaB signalling, PLoS One 8 (2013) e63852.

[31] M. Schmolke, B. Manicassamy, L. Pena, T. Sutton, R. Hai, Z.T. Varga, B.G. Hale, J. Steel, D.R. Perez, A. Garcia-Sastre, Differential contribution of PB1-F2 to the virulence of

highly pathogenic H5N1 influenza A virus in mammalian and avian species, PLoS Pathog 7 (2011) e1002186.

**Figure Legends**

**Figure 1.** Full-length, N- and C-terminal part of PB1-F2 can form amyloid-like structures. (A) Tryptophan fluorescence of PB1-F2 proteins showing blue shift of λmax upon addition of SDS (0.05%w/v) in 10 mM sodium acetate buffer, pH 5. (B) Size distribution of PB1-F2 proteins after addition of 0.005 %w/v SDS to the buffer solution followed by real-time DLS analysis. (C) ThT fluorescence (at 482 nm) real-time recording during PB1-F2 oligomerization to amyloid-like structures upon addition of SDS (0.005 %w/v). (D) AFM images of PB1-F2 structures formed in 0.005 %w/v SDS, 10 mM sodium acetate buffer, pH 5. Concentration of protein was 10 µM. Note that long straight fibrils were only observed with full-length PB1-F2.

**Figure 2.** Cholesterol and cardiolipin effects on PB1-F2 membrane lytic activities. Calcein release from liposomes of various lipid compositions was monitored upon addition of different PB1-F2 forms in concentration ranging from 2 nM to 1 µM. Measurements were done in 10 mM sodium-acetate buffer, pH 5 at room temperature. Error bars indicate the SEM for n = 3-4.

Graphical Abstract

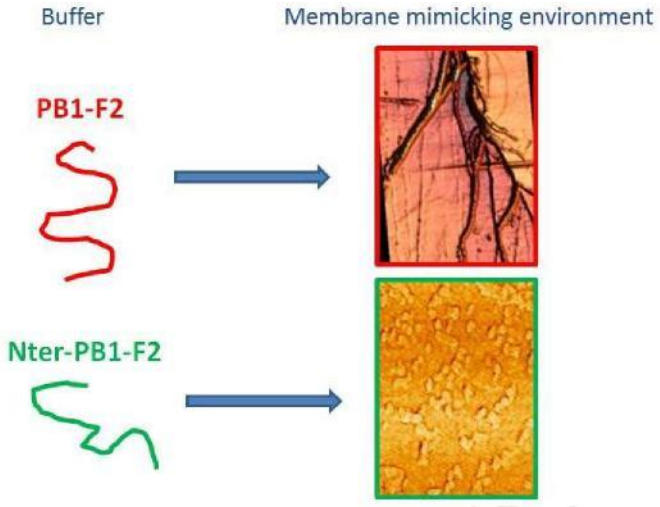

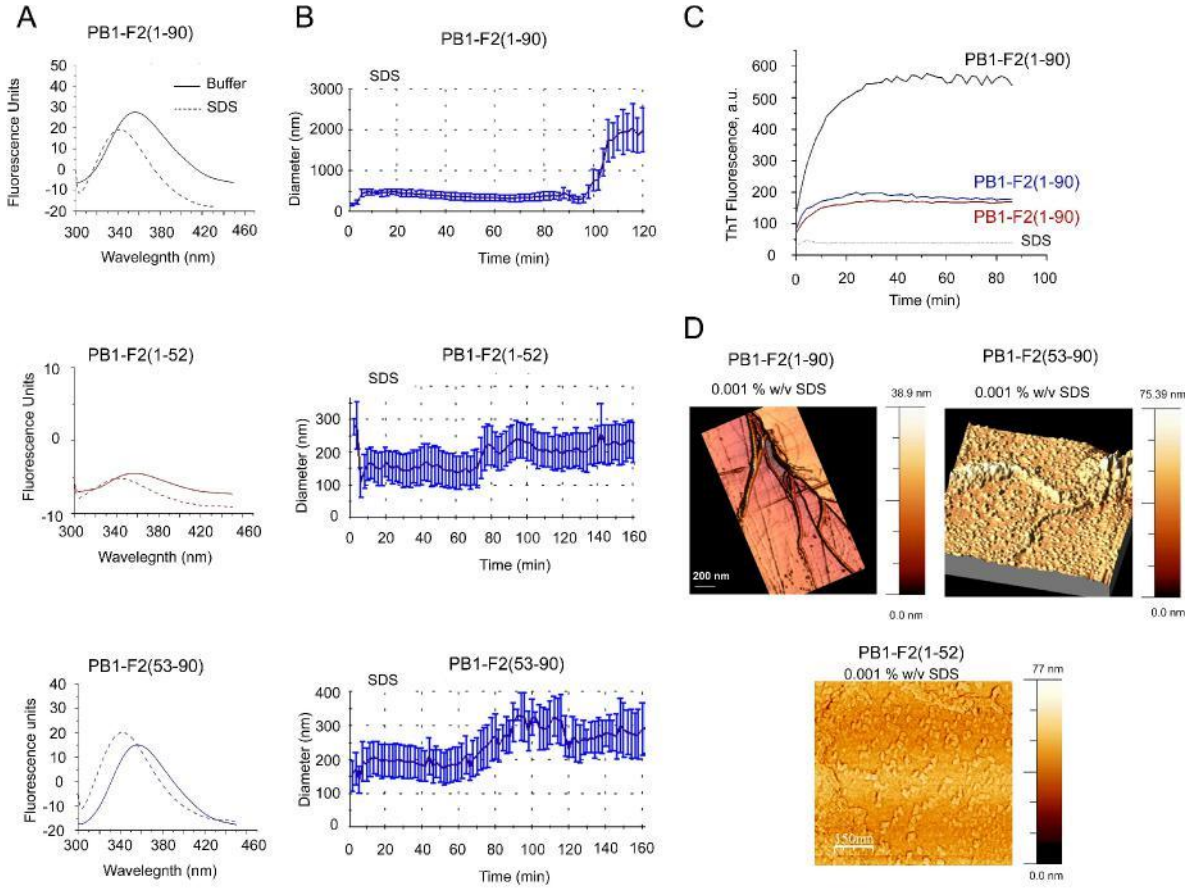

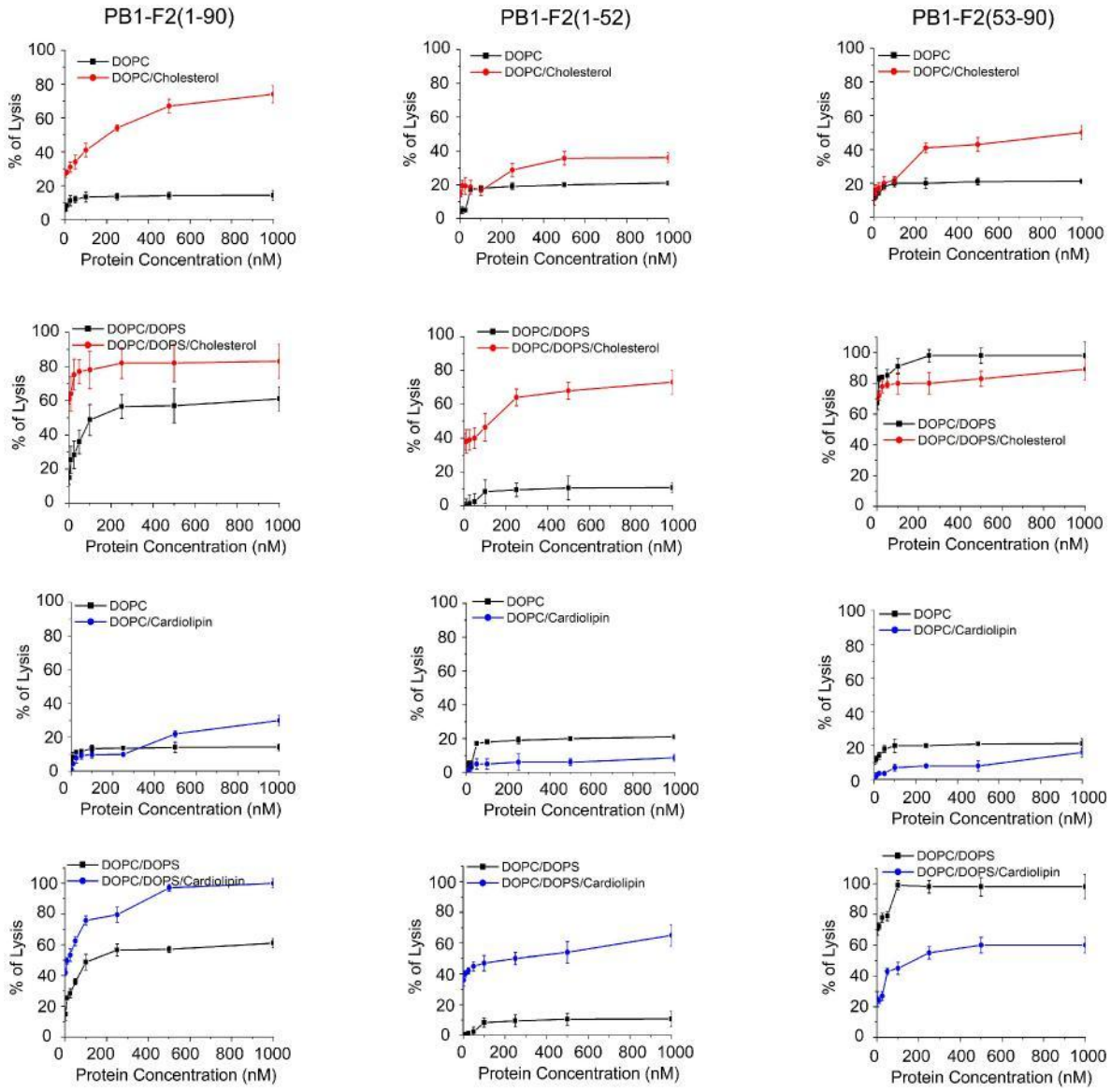

**Highlights**

- **Truncation of PB1-F2 protein of Influenza A viruses modifies its membrane lytic activity.**

- **Truncation of PB1-F2 modifies the protein supramolecular organization in a membrane mimicking environment.**

- **PB1-F2(1-52) can permeabilize liposomes containing cholesterol and cardiolipin while full-length PB1-B2(1-90) efficiently damages anionic liposomes of various lipid compositions.**